Organic Geochemistry 176 (2023) 104526

Contents lists available at ScienceDirect

Organic Geochemistry

journal homepage: www.elsevier.com/locate/orggeochem

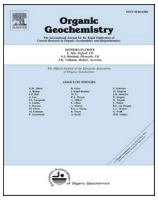

Evaluation of iGDGT carbon isotope fractionation in high performance liquid chromatography

Katherine J. Keller *, Samuel R. Phelps, Ann Pearson

Harvard University, Dept. of Earth & Planetary Sci., 20 Oxford St., Cambridge, MA 02138, United States

ARTICLE INFO

Associate Editor — Rienk Smittenberg

Keywords:
GDGTs
Carbon isotope fractionation
HPLC

ABSTRACT

Careful assessment of fractionation associated with High Performance Liquid Chromatography (HPLC) is essential for ensuring accurate carbon isotope ratio ($\delta^{13}C$) measurements. Here we report these effects for orthogonal dimensions of HPLC separation of iGDGTs. We observe ^{13}C fractionation during normal phase separations using an amino-bonded stationary phase, finding that the heavy isotope preferentially elutes relative to its lighter counterpart, while negligible fractionation occurs during reverse phase HPLC. We argue that the fractionation during normal phase is caused by diminished Van der Waals attraction between ^{13}C-enriched iGDGTs and the stationary phase and appears to depend on the structure of the analyte. Ultimately, these results emphasize the necessity of complete peak collection to preserve the isotopic character of iGDGTs.

1. Introduction

Stable carbon isotopes of organic lipid biomarkers are valuable tools in environmental and paleoclimate research. Specifically, compound-specific $\delta^{13}C$ measurements of archaeal isoprenoid glycerol dialkyl glycerol tetraethers (iGDGTs) and their biphytane derivatives provide important insight into sedimentary methane oxidation (e.g., Pancost et al., 2001; Wakeham et al., 2004; Yoshinaga et al., 2015), marine carbon cycling (e.g., Elling et al., 2019), as well as the provenance of iGDGTs in the environmental and geologic record (e.g., Pearson et al., 2016; Zhu et al., 2021). Generating $\delta^{13}C$ data for iGDGTs or their associated biphytanes requires extensive preparation of lipid extracts prior to isotopic analysis, including multiple steps of HPLC to isolate and purify compounds. Previous research has identified fractionation during HPLC for a variety of compounds and isotope systems (Baumann et al., 1992; Caimi and Brenna, 1997; Iyer et al., 2004; Smittenberg and Sachs, 2007; Julien et al., 2021), but the influence of HPLC on ^{13}C fractionation of iGDGTs has not been reported.

Specific mechanisms responsible for isotope effects during HPLC remain disputed, with arguments invoking properties of the analyte, stationary/mobile phase interactions, or a combination of these factors (Godin et al., 2007). Conventionally, the heavy isotope is preferentially retained on the column relative to the light isotope in normal phase (NP-) HPLC, with the opposite effect generally seen in reverse phase (RP-) HPLC, but some studies have reported diverging patterns relative to this convention (Caimi and Brenna, 1997, and references therein). Prior research has argued that these isotope effects result from diminished non-covalent interactions between the non-polar components of HPLC – mobile phase in NP-HPLC and stationary phase in RP-HPLC – and heavy isotopes (Caimi and Brenna, 1997; Smittenberg and Sachs, 2007). More recent studies instead argue that fractionation in NP-HPLC is attributed to isotopically selective interactions between stationary phase and the analyte, which impact the migration of isotopically substituted compounds in the column (Julien et al., 2021). Understanding how HPLC systems may cause fractionation is essential for evaluating experimental setup and data quality, especially as $\delta^{13}C$ measurements of iGDGT biomarkers play an increasing role in environmental and paleoclimate research. Here, we assess isotope effects associated with GDGT separation for NP- and RP-HPLC and document the magnitude and timing of ^{13}C fractionation across peak elution during NP-HPLC.

2. Methods

2.1. Samples and materials

Synthetic and environmental standards were used as test samples. Carolina Margin crenarchaeol (CM-cren; m/z 1292), was previously isolated and purified (Pearson et al., 2016). Synthetic iGDGT analog, C_{46}-GTGT (m/z 744), was assessed as an acyclic, non-isoprenoid alternative to CM-cren. Experiments were performed for both compounds

* Corresponding author.
E-mail address: katherinekeller@g.harvard.edu (K.J. Keller).

https://doi.org/10.1016/j.orggeochem.2022.104526
Received 31 July 2022; Received in revised form 28 October 2022; Accepted 30 October 2022
Available online 4 November 2022

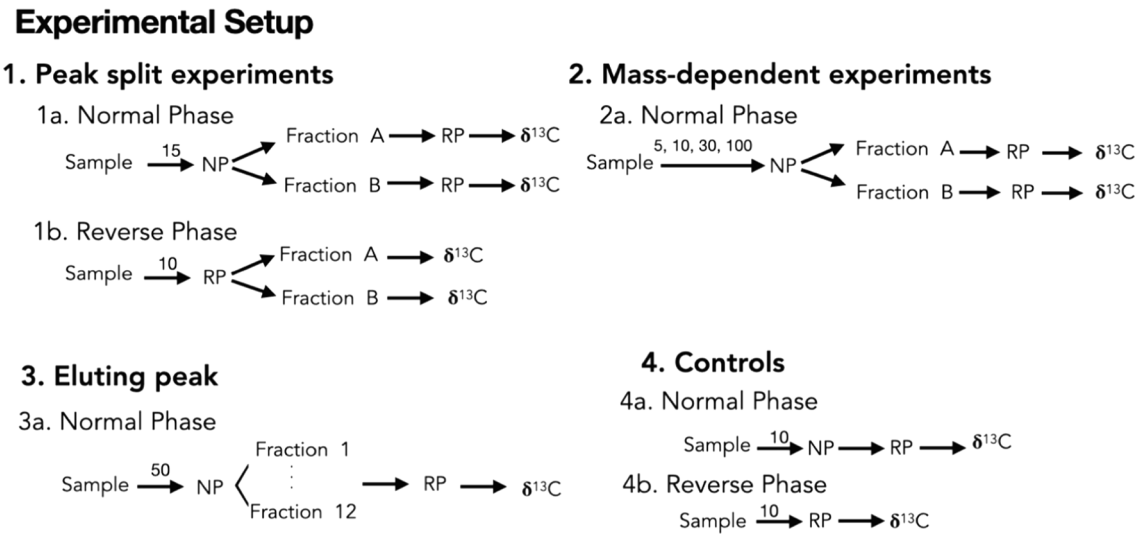

Fig 1. Flowchart of steps for each experiment, showing the starting masses of analyte (μgC).

using an Agilent 1200 series HPLC. Agilent analytical ZORBAX amino-column (NH_2–, 4.6x250 mm, 5 μm, p.n. 880952–708) and analytical ZORBAX Eclipse XDB-C8 column (C8-, 4.6x150 mm, 5 μm, p.n. 993967–906) were used for NP- and RP-HPLC, respectively.

2.2. NP- and RP-HPLC

The experimental setup mimicked protocols used to measure $\delta^{13}C$ values of environmental iGDGTs (Fig. 1), treating the standards used here in a similar manner to environmental samples described in previous studies (Pearson et al., 2016). iGDGT compounds were collected isocratically with 98:2 hexane: isopropanol mixture at a 1 ml/min flow rate for NP-HPLC experiments; other program details follow procedures described by Pearson et al., 2016. Injection volumes were 95 μl, containing 5–100 μg of sample material (Fig. 1); typically, injected sample material is limited to a maximum amount of 20 μg (Pearson et al., 2016). Concentrations were measured before and after NP-HPLC steps by flow injection analysis (FIA), monitoring *m/z* 300–1350, relative to a dilution series of C_{46}-GTGT standard (Huguet et al., 2006). Following NP-HPLC collection, samples were further purified by RP-HPLC by dissolving in 65:35 ethyl acetate: acetonitrile. Injection volumes were 95 μl, and sample amounts were limited to 1–10 μg of material to avoid column overloading. Compounds eluted in a gradient of acetonitrile, water and ethyl acetate, as detailed previously (Ingalls et al., 2006; Shah et al., 2008; Pearson et al., 2016). Three fractions were collected and analyzed for $\delta^{13}C$: the preceding minute (F1), the eluting compound (F2), and the trailing minute (F3).

2.3. Peak collection

We conducted three experiments: **(1)** Eluting CM-cren and C_{46}-GTGT peaks were collected as front (A) and back (B) fractions of roughly equal concentrations during NP- and RP-HPLC for analysis of concentrations and $\delta^{13}C$ ratios. For each experiment, complete peaks also were collected as non-fractionated controls. **(2)** NP-HPLC was repeated for the A/B experiments using varying amounts of C_{46}-GTGT (ranging from 5 to 100 μg; Table 1) **(3)** In a final trial, a single injection of C_{46}-GTGT was divided into 12 contiguous collection windows to allow temporal resolution of $\delta^{13}C$ ratios.

2.4. $\delta^{13}C$ isotope analysis

Measurements of $\delta^{13}C$ were obtained by Spooling Wire Microcombustion IRMS (SWiM-IRMS) following Pearson et al. (2016). All data are reported relative to Vienna Pee Dee Belemenite (VPBD) and standardized to the same reference frame using CO_2 reference gas and master aliquots of C_{46}-GTGT and CM-cren (−30.3 ‰ and –18.5 ‰, respectively; Pearson et al., 2016). Dilution series of C_{46}-GTGT and CM-cren standards were used to quantify and correct for the measurement blank (intersection of $\delta^{13}C$ vs 1/mass) and this method yielded similar results to direct measurement of authentic process blanks (HPLC-collected 1-ml aliquots). The average $\delta^{13}C$ value of the blank was −29.7 ‰; if the $\delta^{13}C$ value could not be determined for a given series, a default value of −30 ‰ was imposed. The mass of the blank was *ca.* 1–1.5 ngC/injection, resulting in average blank contribution of 2 % (average injection, *ca.* 50 ngC). Between 6 and 8 replicate measurements were made of the F2 (iGDGT) sample. Outliers were removed by Q test (95 % confidence interval), and results were averaged. After isotopic analysis, the purity of any remaining material was assessed by FIA.

3. Results

Nearly equal quantities of material were obtained in the respective A and B splits for each peak (Table 1), and these estimated concentrations (μg C) were used to calculate mass balance together with the $\delta^{13}C$ values. The cumulative isotope ratios are within 0.35 ‰ of the starting material indicating the peaks were completely collected in the A and B fractions. Negligible differences between A and B ($\Delta\delta = \delta^{13}C_A - \delta^{13}C_B$) were observed during RP-HPLC (Fig. 2A). However, larger Δδ values were observed during NP-HPLC, with ^{13}C-enriched molecules preferentially accumulating in the A fractions (Fig. 2B); a two-tailed *t*-test confirms these differences are significant ($p < 0.05$). While the direction of the effect is the same for both analytes, their Δδ values vary, with smaller Δδ values for CM-cren compared to C_{46}-GTGT by nearly a factor of 2. This difference between the analytes suggests that the extent of fractionation depends, at least in part, on the structure of the analyte.

To assess how the isotope effect responds to the amount of analyte loaded onto the column during NP-HPLC, varying amounts (5–100 μg) of the C_{46}-GTGT were injected, and A and B fractions again were analyzed. Larger Δδ values were observed when smaller amounts of sample were injected (Fig. 2C; Table 1). This observation suggests the surface-active sites of the stationary phase are isotopically selective. It appears that increased occupation of binding sites when more material is on the column reduces the interactions between the analyte and stationary phase, resulting in a smaller Δδ between A and B fractions.

To explore this further, $\delta^{13}C$ measurements were made at twelve successive intervals across a single eluting C_{46}-GTGT peak (Fig. 3; Table 2). The values of $\delta^{13}C$ range from ~ –26 ‰ in fraction 3 to < –32

Table 1
Mass and isotope data from HPLC separation experiments.

Compound	Mass (μg)	Fraction	LC mode	$\delta^{13}C$ (‰)	% of Peak	$\Delta\delta_{A-B}$ (‰)
CM-cren	10	A	RP	−18.0 ± 0.3	58.8	
		B	RP	−18.6 ± 0.2	41.2	
Weighted avg				−18.3 ± 0.2		0.6
CM-cren	15	A	NP	−17.3 ± 0.4	44.7	
		B	NP	−18.8 ± 0.2	55.3	
Weighted avg				−18.2 ± 0.3		1.6
C_{46} -GTGT	10	A	RP	−30.2 ± 0.2	54.6	
		B	RP	−30.4 ± 0.1	45.4	
Weighted avg				−30.3 ± 0.2		0.3
C_{46} -GTGT	15	A	NP	−28.6 ± 0.1	42.7	
		B	NP	−31.9 ± 0.1	57.3	
Weighted avg				−30.5 ± 0.1		3.3
C_{46} -GTGT	5	A	NP	−28.2 ± 0.2	41.2	
		B	NP	−31.7 ± 0.3	58.8	
Weighted avg				−30.3 ± 0.2		3.5
C_{46} -GTGT	10	A	NP	−28.1 ± 0.2	35.2	
		B	NP	−31.5 ± 0.2	63.9	
Weighted avg				−30.0 ± 0.2		3.4
C_{46} -GTGT	30	A	NP	−29.5 ± 0.3	70.4	
		B	NP	−32.0 ± 0.6	29.6	
Weighted avg				−30.2 ± 0.4		2.5
C_{46} -GTGT	100	A	NP	−29.8 ± 0.7	57.6	
		B	NP	−32.0 ± 0.1	42.4	
Weighted avg				−30.8 ± 0.5		2.2
C_{46} GTGT (unsplit)	10			−30.2 ± 0.3		
C_{46} GTGT true *				−30.3 ± 0.3		
CM-cren (unsplit)	10			−18.6 ± 0.1		
CM-cren true*				−18.5 ± 0.3		

* Determined by closed-tube combustion/dual-inlet IRMS combustion. (Pearson et al., 2016).

‰ in fractions 7–10, but cumulatively sum to the correct total (blue squares, Fig. 3). We assume the slight ^{13}C enrichment in fractions 1 + 2 and 11 + 12 is due to a combination of the small sample size and lower purity for these terminal fractions, i.e., a background state of minimal, but non-zero, column bleed. The resolution of the two isotopes is pronounced: fraction 3 (~7% peak mass) and fraction 9 (~5% peak mass) are 4 ‰ enriched and 2.5 ‰ depleted relative to the true $\delta^{13}C$ value of C_{46}-GTGT, respectively. Calculation of a mixture of Gaussian peaks representing mono-^{13}C-substituted C_{46}-GTGT and its all-^{12}C isotopologue (with $\delta^{13}C$ = -30.3 ‰ for the net mixture) indicates the effect on elution time of harboring a ^{13}C substitution is ~ 0.1 *sec* for this 46-carbon molecule (Fig. 3). While this seems vanishingly small, if viewed on a per-carbon basis (assuming individual C—C interactions with the column), it is equivalent to a 5 *sec* delay for a ^{12}C compared to a ^{13}C. More importantly, it points to the critical importance of collecting complete peaks during NP-HPLC. The populations of the two isotopologues needed to create the total ^{13}C content (−30.3 ‰) are approximately equal, and thus unlike gas chromatography-IRMS, this implies that the molecule containing the heavy isotope has a peak area nearly the same as the light isotope. In GC-IRMS separations ^{13}C is distributed heavily towards the leading CO_2 shoulder (1 % $^{13}CO_2$ preceding 99 % $^{12}CO_2$ for the combustion gases of GC-IRMS), while for HPLC the elution represents nearly synchronous peaks of equal size (i.e., is front-loaded only in the case of doubly substituted isotopologues and/or "clumping"). Thus, it is crucial to collect the entire peak.

4. Discussion

Preferential elution of ^{13}C-enriched compounds differs from some earlier works, although these studies evaluated different compounds, isotope systems, and HPLC methods and therefore may not be analogous. For example, Smittenberg and Sachs (2007) assessed $\delta^{2}H$ fractionation of cholesterol eluting in a gradient of dichloromethane and hexane during NP-HPLC and found that the lighter isotope eluted earlier. Differences in lengths of C-^{2}H and C-^{1}H bonds were invoked to explain decreased polarizability of the heavy isotope and a concomitant reduction in interation with the mobile phase. Iyer et al. (2004) observed the same pattern of elution for deuterated and non-deuterated heterocyclic compounds, but attributed the order of elution to preferential binding of deuterated compounds with the stationary phase (i.e., higher binding energies).

Our experiments align with the idea of a dominant role for the stationary phase in generating these isotope effects. In the present work, increases in analyte loading decrease Δδ, pointing to a decrease in interaction time between the analyte and stationary phase at high sample concentration (activity). Intramolecular bonds involving ^{13}C have shortened bond lengths. This decreases polarizability and may weaken, rather than strengthen, interactions with the stationary phase, resulting in poor retention of the heavy isotope; excess material on-column diminishes this effect. While both our study and Smittenberg and Sachs (2007) invoke similar bond-energy arguments, the differing elution order of isotopes indicates there can be either a stronger influence of the mobile phase on the analyte (Smittenberg and Sachs, 2007) or of the stationary phase on the analyte (this study). This suggests that unlike the predictable isotopic resolution of gas chromatography-IRMS (with temperature as the primary variable), HPLC separations each should be evaluated separately for their impact on isotopic sorting.

The effect of the molecular structure of the analyte is further demonstrated by differences in Δδ values between CM-cren and C_{46}-GTGT. Despite using the same elution conditions, a more pronounced isotope effect was observed for acyclic C_{46}-GTGT compared to heterocyclic CM-cren. While it is possible the magnitude of Δδ may be related to the polarity difference between analyte and stationary phase (C_{46}-GTGT is less polar than crenarchaeol and spends less time on-column), more likely the diminished fractionation is due to isotope combinatorial effects. Because 1:100 carbon atoms are ^{13}C, there will be approximately-one ^{13}C in every-two C_{46}-GTGTs, leading to nearly equal populations of substituted and un-substituted molecules (assuming a reasonably stochastic distribution of ^{13}C). This yields the maximum possible isotopic sorting on-column (Fig. 3). By contrast, the majority of all C_{86}-iGDGTs should contain at least one ^{13}C, with smaller populations containing two or zero, collectively suppressing the sorting effect (Fig. 3).

5. Conclusions

NP-, but apparently not RP-, separation of iGDGTs by HPLC significantly fractionates the stable carbon isotopes, with preferential elution

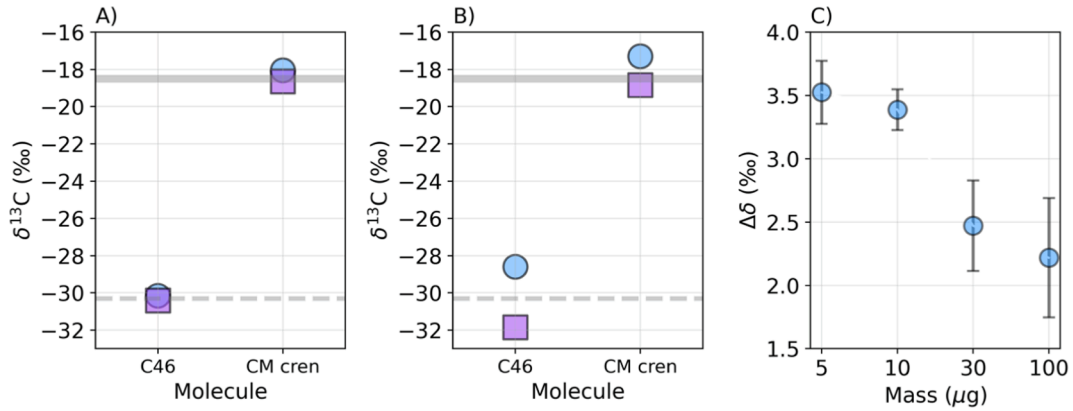

Fig 2. Carbon isotope ratios of fractions A (circles) and B (squares) of C_{46} GTGT and CM-cren separated by A) reverse phase- (C8-) and B) normal phase- (NH_2–) HPLC. The dashed line and gray bar represent the true $\delta^{13}C$ values for C_{46} GTGT and CM-cren, respectively. $N = 1$ authentic replicate preparations; $n = 6$–8 repeat measurements for each replicate. Error bars are smaller than symbols. C) Quantity effects on Δδ between A and B fractions of C_{46}-GTGT during NP-HPLC.

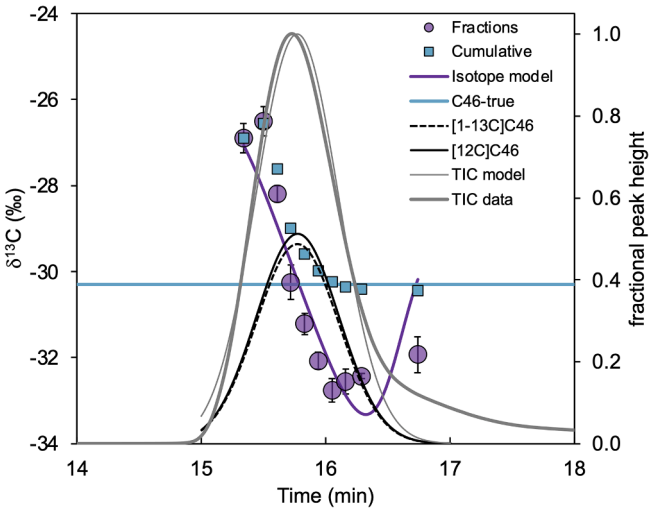

Fig 3. Resolution of $\delta^{13}C$ values for C_{46}-GTGT fractions (purple circles) collected by NP-HPLC, along with the cumulative $\delta^{13}C$ value of the total recovered material (−30.4 ‰; blue squares). The total ion chromatogram (TIC; thick grey line) was modeled as a mixture (0.488:0.512; equivalent to $\delta^{13}C$ = -30.3 ‰ total) of Gaussian peaks of mono-^{13}C- and all-^{12}C-isotopologues (black lines). The total of these peaks (thin grey line) mimics the values and temporal resolution of the $\delta^{13}C$ data (purple line), and indicates the ^{13}C sorting reflects retention time differences of < 0.002 min.

of ^{13}C relative to ^{12}C. This demonstrates the importance of complete collection of eluting iGDGT molecules during NP-HPLC. Further work is required to test whether these principles also apply to $^{2}H/^{1}H$ ratios, and whether similar fractionation associated with HPLC pertains to other organic compounds commonly used in isotope geochemistry such as fatty acids and amino acids.

Declaration of Competing Interest

The authors declare that they have no known competing financial interests or personal relationships that could have appeared to influence the work reported in this paper.

Data availability

Experimental data are included in supplementary Excel file

Table 2
Carbon isotope values across an eluting C_{46}-GTGT peak during NP-HPLC.

Fraction	~Amount (μg)	Estimated % of Total	Collection Window (min)	$\delta^{13}C$ (‰)
1/2*	0.6	1.0	15.3 – 15.5	−26.9 ± 0.3
3	4.1	7.4	15.5 – 15.6	−26.5 ± 0.3
4	8.7	15.6	15.6 – 15.7	−28.2 ± 0.2
5	14.8	26.5	15.7 – 15.8	−30.3 ± 0.4
6	10.4	18.7	15.8 – 15.9	−31.2 ± 0.2
7	7.3	13.0	15.9 – 16.1	−32.1 ± 0.2
8	4.4	7.9	16.1 – 16.2	−32.8 ± 0.3
9	2.8	5.1	16.2 – 16.3	−32.6 ± 0.3
10	1.3	2.4	16.3 – 16.4	−32.4 ± 0.1
11/12	1.4	2.4	16.4 – 16.7	−31.9 ± 0.4

* Fractions below quality threshold with < 1 μg of sample material.

Acknowledgements

We thank the Associate Editor, Rienk Smittenberg, and two anonymous reviewers for their valuable feedback. Funding was provided by Harvard University and the National Science Foundation, United States (award 1843285 to A.P.).

Appendix A. Supplementary data

Supplementary data to this article can be found online at https://doi.org/10.1016/j.orggeochem.2022.104526.

References

Baumann, P.Q., Ebenstein, D.B., O'Rourke, B.D., Nair, K.S., 1992. High-performance liquid chromatographic technique for non-derivatized leucine purification: evidence for carbon isotope fractionation. Journal of Chromatography B 573, 11–16.
Caimi, R.J., Brenna, J.T., 1997. Quantitative evaluation of carbon isotopic fractionation during reversed-phase high-performance liquid chromatography. Journal of Chromatography A 757, 307–310.
Elling, F.J., Gottschalk, J., Doeana, K.D., Kusch, S., Hurley, S.J., Pearson, A., 2019. Archaeal lipid biomarker constraints on the Paleocene-Eocene carbon isotope excursion. Nature Communications 10, 1–10.

Godin, J.P., Fay, L.B., Hopfgartner, G., 2007. Liquid chromatography combined with mass spectrometry for ^{13}C isotopic analysis in life science research. Mass Spectrometry Reviews 26, 751–774.
Huguet, C., Hopmans, E.C., Febo-Ayala, W., Thompson, D.H., Sinninghe Damsté, J.S., Schouten, S., 2006. An improved method to determine the absolute abundance of glycerol dibiphytanyl glycerol tetraether lipids. Organic Geochemistry 37, 1036–1041.
Ingalls, A.E., Shah, S.R., Hansman, R.L., Aluwihare, L.I., Santos, G.M., Druffel, E.R.M., Pearson, A., 2006. Quantifying archaeal community autotrophy in the mesopelagic ocean usinq natural radiocarbon. Proceedings of the National Academy of Sciences USA 103, 6442–6447.
Iyer, S.S., Zhang, Z.P., Kellogg, G.E., Karnes, H.T., 2004. Evaluation of deuterium isotope effects in normal-phase LC-MS-MS separations using a molecular modeling approach. Journal of Chromatographic Science 42, 383–387.
Julien, M., Liégeois, M., Höhener, P., Paneth, P., Remaud, G.S., 2021. Intramolecular non-covalent isotope effects at natural abundance associated with the migration of paracetamol in solid matrices during liquid chromatography. Journal of Chromatography A 1639, 461932.
Pancost, R.D., Hopmans, E.C., Sinninghe Damsté, J.S., 2001. Archaeal lipids in mediterranean cold seeps: Molecular proxies for anaerobic methane oxidation. Geochimica et Cosmochimica Acta 65, 1611–1627.
Pearson, A., Hurley, S.J., Walter, S.R.S., Kusch, S., Lichtin, S., Zhang, Y.G., 2016. Stable carbon isotope ratios of intact GDGTs indicate heterogeneous sources to marine sediments. Geochimica et Cosmochimica Acta 181, 18–35.
Shah, S.R., Mollenhauer, G., Ohkouchi, N., Eglinton, T.I., Pearson, A., 2008. Origins of archaeal tetraether lipids in sediments: Insights from radiocarbon analysis. Geochimica et Cosmochimica Acta 72, 4577–4594.
Smittenberg, R.H., Sachs, J.P., 2007. Purification of dinosterol for hydrogen isotopic analysis using high-performance liquid chromatography-mass spectrometry. Journal of Chromatography A 1169, 70–76.
Wakeham, S.G., Hopmans, E.C., Schouten, S., Sinninghe Damsté, J.S., 2004. Archaeal lipids and anaerobic oxidation of methane in euxinic water columns: A comparative study of the Black Sea and Cariaco Basin. Chemical Geology 205, 427–442.
Yoshinaga, M.Y., Lazar, C.S., Elvert, M., Lin, Y.S., Zhu, C., Heuer, V.B., Teske, A., Hinrichs, K.U., 2015. Possible roles of uncultured archaea in carbon cycling in methane-seep sediments. Geochimica et Cosmochimica Acta 164, 35–52.
Zhu, Q.Z., Elvert, M., Meador, T.B., Becker, K.W., Heuer, V.B., Hinrichs, K.U., 2021. Stable carbon isotopic compositions of archaeal lipids constrain terrestrial, planktonic, and benthic sources in marine sediments. Geochimica et Cosmochimica Acta 307, 319–337.